# FREQUENCY-DOMAIN ITERATIVE MUI CANCELLATION FOR DUOBINARY PARTIAL RESPONSE FILTERED SC-FDMA UPLINK

**Kohei Abo, Amnart Boonkajay, Fumiyuki Adachi**

Dept. of Communications Engineering, Graduate School of Engineering, Tohoku University versity
6-6-05 Aza-Aoba, Aramaki, Aoba-ku, Sendai 980-8579 Japan
abo@mobile.ecei.tohoku.ac.jp, amnart@mobile.ecei.tohoku.ac.jp, adachi@ecei.tohoku.ac.jp

**Abstract:** Duobinary partial response (PR) filtered single-carrier frequency-domain multi-access (SC-FDMA) uplink has a potential to achieve higher spectral efficiency (SE) by allowing spectrum overlapping between adjacent users. However, strong multiuser interference (MUI) degrades the bit-error rate (BER) and throughput performances. In this paper, we present two types of frequency-domain MUI cancellation technique for duobinary PR filtered SC-FDMA, which are frequency-domain iterative parallel MUI cancellation (FD-IPMUIC) and frequency-domain iterative successive MUIC (FD-ISMUIC). A series of minimum mean-square error based frequency-domain equalization (MMSE-FDE), FD-MUIC, and soft-decision decoding using soft output Viterbi algorithm (SOVA) is repeated for a sufficient number of times. By using the SOVA, MMSE-FDE weight and MUI replica are updated. Computer simulation results show that both the BER performance and SE can be improved.

**Keywords:** Duobinary PR filter, SC-FDMA, frequency-domain MUI cancellation, MMSE-FDE, Soft output Viterbi algorithm

## 1 Introduction

Broadband wireless channel is composed of many propagation paths having different time delays. This makes the channel become frequency-selective, in which inter-symbol interference (ISI) degrades the system performance of single-carrier (SC) transmission in terms of bit error rate (BER) [1]. Minimum mean-square error based frequency-domain equalization (MMSE-FDE) can suppress the ISI while obtaining the frequency diversity gain [2-4]. Square-root Nyquist filter is typically used as ISI-free transmit/receive filters in the SC transmission system [5]. However, as the filter roll-off factor increases, the required transmission bandwidth increases, leading to the degradation of spectral efficiency (SE). By using partial response (PR) filter to permit filter-controlled ISI, higher SE is achieved [1, 6]. Recently, we studied point-to-point duobinary PR filtered SC transmission and showed that the use of maximum likelihood sequence estimation (MLSE) can effectively mitigate the ISI caused by duobinary PR filter and has only a slight BER performance degradation compared to square-root Nyquist filter [7].

Since SC signal has much lower peak-to-average power ratio (PAPR) than orthogonal frequency division multiplexing (OFDM) signal, SC with FDE is more attractive for uplink transmission, and SC frequency-domain multi-access (SC-FDMA) with FDE is adopted in LTE systems. Duobinary PR filtering can also be applied to SC-FDMA uplink to achieve higher SE by allowing spectrum overlapping between adjacent users. However, strong multiuser interference (MUI) occurs due to spectrum overlapping degrades the BER and throughput performances. In Ref. [8], iterative MUI cancellation (MUIC) is proposed for square-root Nyquist filtered SC-FDMA with spectrum overlapping, in which the bandwidth per user is kept $1/T_s$ irrespective of the roll-off factor, where $1/T_s$ is the per-user symbol rate. When using the duobinary PR filtering, the per-user bandwidth can be made narrower than square-root Nyquist filtering case.

In this paper, we propose two types of frequency-domain MUI cancellation (FD-MUIC) for duobinary PR filtered SC-FDMA uplink. The first one is frequency-domain iterative parallel MUIC (FD-IPMUIC), in which a series of MMSE-FDE, FD-MUIC [8], and soft-decision decoding using soft output Viterbi algorithm (SOVA) [9,10] is repeated a sufficient number of times. The second one is frequency-domain iterative successive MUIC (FD-ISMUIC), in which users are ranked according to their instantaneous received signal-to-interference plus noise power ratios (SINRs), then the cancellation is performed successively beginning from the user having the largest SINR. MMSE-FDE and MUIC can mitigate ISI caused by channel frequency-selectivity and MUI, respectively, while the use of SOVA mitigates the filter-controlled ISI. MMSE-FDE weight and MUI replica are updated for the next iteration after performing SOVA. Throughput performance of duobinary PR filtered SC-FDMA using the proposed MUIC is expected to be better than square root Nyquist filtered SC-FDMA.

The remainder of this paper is organized as follows. In Sect. 2, transmission system model is presented. In Sect. 3, MUIC is presented. In Sect. 4, computer simulation results are shown in aspect of BER performance and throughput performance. Finally, Sect. 5 concludes the paper.

**978-1-4799-4734-8 /14/$31.00 ©2014 IEEE**

## 2 Transmission system

SC-FDMA uplink transmitter and receiver model is illustrated by Fig. 1. Throughout the paper, symbol-spaced discrete-time signal representation is considered.

A block of data-modulated symbols of the $u$-th user ($u$=0,…,$U$–1), represented by $\{d_u(n);\ n=0\sim N_{tx}-1\}$, is transformed into $N_{tx}$ frequency-domain components $\{D_u(k);\ k=0\sim N_{tx}-1\}$ by employing $N_{tx}$-point discrete Fourier transform (DFT). The duobinary PR filter is implemented in the frequency domain, where its filter coefficients are denoted by $\{W_T(k);\ k=-N_{tx}/2\sim N_{tx}/2-1\}$ and $W_T(k)$ is given by Ref. [1]

$$W_T(k)=\sqrt{2}\cos(k\pi/N_{tx})\exp(-jk\pi/N_{tx}) \tag{1}$$

Filtered frequency-domain signal is denoted by $\{S_u(k)=W_T(k-N_{tx}/2)D_u(k);\ k=0\sim N_{tx}-1\}$, and the corresponding time-domain transmit signal after duobinary PR filtering $s_u(n)$ can be expressed as

$$s_u(n)=\sqrt{1/2}\left(d_u(n)+d_u((n-1)\bmod N_{tx})\right) \tag{2}$$

Localized mapping, as illustrated in Fig. 2(a), is considered in this paper. A parameter $\beta=[N_c-m(U-1)]/N_c$, where $m=0,1,\ldots,N_{tx}/2$ and $\beta$ is between $0.5+N_{tx}/N_c$ and 1, is defined in order to describe the spectrum overlapping between adjacent users. If $\beta$ is small, spectrum overlapping is denser, thereby improving the SE. Frequency-domain signal of the $u$-th user after spectrum mapping $\{S'_u(k);\ k=0\sim N_c-1\}$ can be expressed as

$$S'_u(k)=\begin{cases}S_u(k-u(N_{tx}-m)),\\ u(N_{tx}-m)\le k\le u(N_{tx}-m)+N_{tx}-1\\ 0\quad otherwise\end{cases} \tag{3}$$

After that, $N_c$-point inverse fast Fourier transform (IFFT) is applied to $S'_u(k)$, yielding time-domain transmit signal $\{s'_u(n);\ n=0\sim N_c-1\}$ with

$$s'_u(n)=\sqrt{2E_{s.u}/T_s}\sqrt{1/N_c}\sum_{k=0}^{N_c-1}S'_u(k)\exp(j2\pi nk/N_c) \tag{4}$$

where $E_{s,u}$ denote the symbol energy of the $u$-th user. To avoid the inter-block interference (IBI), the last $N_g$ samples of each transmission block are copied as a cyclic prefix (CP) and inserted into the guard interval (GI) placed at the beginning of each bock. The CP length needs to be longer than the maximum time delay of the channel. In this paper, we assume that $U=N_c/N_{tx}$ users simultaneously access the same base station.

The transmit signal of each user goes through a wireless channel having the following channel impulse response $h_u(\tau)$ and is received by a base station receiver. $h_u(\tau)$ can be expressed as

$$h_u(\tau)=\sum_{l=0}^{L-1}h_{u,l}\delta(\tau-\tau_l) \tag{5}$$

where $\tau_l$ is the delay time and $h_{u,l}$ is the complex-valued path gain of the $l$-th path with $E[\sum_{l=0}^{L-1}|h_{u,l}|^2]=1$. The CP-removed received signal $r(n)$ at the $n$th time instant can be expressed as

$$r(n)=\sum_{u=0}^{U-1}\sum_{l=0}^{L-1}h_{u,l}\cdot s_u(n-l)+\eta(n) \tag{6}$$

where $\eta(n)$ denotes the zero-mean complex-valued

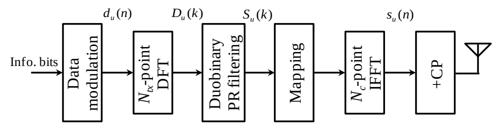


**(a)**Transmitter

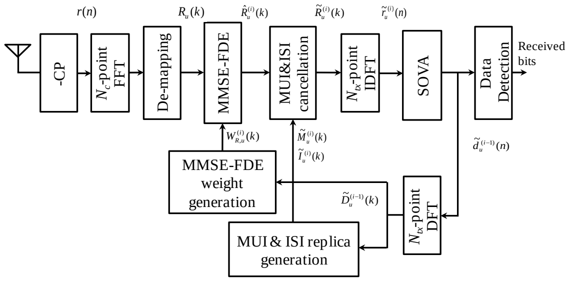


**(b)**Receiver

**Figure 1** Uplink transmission system model of frequency-domain MUIC for duobinary PR filtered SC-FDMA

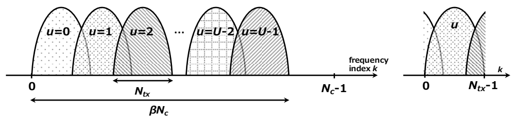


**(a)**Mapping **(b)**De-mapping

**Figure 2** Spectrum mapping and de-mapping

Gaussian noise having variance $2N_0/T_s$ with $N_0$ being the one-sided power spectral density of additive white Gaussian noise (AWGN). $N_c$-point FFT is applied to transform $\{r(n);\ n=0\sim N_c-1\}$ into the frequency-domain received signal $\{R(k);\ k=0\sim N_c-1\}$ with

$$R(k)=\sum_{u=0}^{U-1}\sqrt{2E_{s.u}/T_s}H'_u(k)S'_u(k)+\Pi(k) \tag{7}$$

where

$$\begin{cases}H'_u(k)=\sum_{l=0}^{L-1}h_{u,l}\exp(-j2\pi kl/N_c)\\ \Pi(k)=\sqrt{1/N_c}\sum_{n=0}^{N_c-1}\eta(n)\exp(-j2\pi kn/N_c)\end{cases} \tag{8}$$

Here, $H'_u(k)$ and $\Pi(k)$ are the channel gain and the noise component due to AWGN, respectively. Spectrum de-mapping, as illustrated in Fig. 2(b), is applied to $R(k)$ to obtain the frequency-domain signal $\{R_u(k);\ k=0\sim N_{tx}-1\}$ and channel gain $\{H_u(k);\ k=0\sim N_{tx}-1\}$ of the $u$-th user.

# 3 Iterative MUI cancellation

A series of MMSE-FDE, FD-MUIC, and soft-decision decoding using SOVA is applied to the frequency-domain received signal after de-mapping of each user, either in parallel approach (i.e., cancellation is employed for all users simultaneously) or successive approach (i.e., cancellation is done respectively, beginning from the user having the highest instantaneous received SINR). Cancellation is repeated in a sufficient number of times.

MMSE-FDE, MUIC and SOVA are done iteratively, where MMSE-FDE weight at the *i*-th (*i*=0,1,…,*I*) iteration is given by

$$\begin{aligned}\hat{R}_u^{(i)}(k) &= R_u(k)W_{R,u}^{(i)}(k)\\ &= \sqrt{2E_{s,u}/T_s}\,S_u(k)\hat{H}_u^{(i)}(k)+M_u(k)+\hat{\Pi}^{(i)}(k)\end{aligned} \tag{9}$$

where

$$\begin{cases}\hat{H}_u^{(i)}(k)=H_u(k)W_{R,u}^{(i)}(k)\\ \hat{\Pi}^{(i)}(k)=\Pi(k)W_{R,u}^{(i)}(k)\end{cases} \tag{10}$$

In Eq. (9) and (10), $W_R^{(i)}(k)$ is one-tap FDE weight at the *i*-th iteration, $\hat{H}_u^{(i)}(k)$ and $\hat{\Pi}^{(i)}(k)$ are the equivalent channel gain and the noise component after performing MMSE-FDE at the *i*-th iteration, respectively. The derivation of FDE weight is described in Sect. 3-C.

MUIC at the *i*-th (*i*=0,1,…,*I*) iteration is performed on $\hat{R}_u^{(i)}(k)$ in the frequency-domain as

$$\tilde{R}_u^{(i)}(k)=\hat{R}_u^{(i)}(k)-\tilde{M}_u^{(i)}(k)-\tilde{I}_u^{(i)}(k) \tag{11}$$

where $\tilde{M}_u^{(i)}(k)$ and $\tilde{I}_u^{(i)}(k)$ are MUI replica and residual ISI replica, respectively, which will be described in Sect. 3-B. After the MUI cancellation, $N_{tx}$-point inverse DFT (IDFT) is applied to transform the frequency-domain signal $\{\tilde{R}_u^{(i)}(k);k=0\sim N_{tx}-1\}$ into the time-domain signal $\{\tilde{r}_u^{(i)}(n);n=0\sim N_{tx}-1\}$ for data demodulation, where

$$\begin{aligned}\tilde{r}_u^{(i)}(n)&=\sqrt{1/N_{tx}}\sum_{k=0}^{N_{tx}-1}\tilde{R}_u^{(i)}(k)\exp\left(j2\pi nk/N_{tx}\right)\\ &=A_u^{(i)}s_u(n)+\mu_u^{(i)}(n)+\iota_u^{(i)}(n)+\hat{\eta}_u^{(i)}(n)\end{aligned} \tag{12}$$

with

$$\begin{cases}A_u^{(i)}=\sqrt{2E_{s,u}/T_s}\left(1/N_{tx}\right)\sum_{k=0}^{N_{tx}-1}H_u(k)W_{R,u}^{(i)}(k)\\ \mu_u^{(i)}(n)=\sqrt{1/N_{tx}}\sum_{k=0}^{N_{tx}-1}\left(M_u^{(i)}(k)-\tilde{M}_u^{(i)}(k)\right)\exp\left(j2\pi nk/N_{tx}\right)\\ \iota_u^{(i)}(n)=\sqrt{1/N_{tx}}\sum_{k=0}^{N_{tx}-1}\begin{pmatrix}\left(\sqrt{2E_{s,u}/T_s}\hat{H}_u^{(i)}(k)-A_u^{(i)}\right)\left(D_u(k)-\tilde{D}_u^{(i-1)}(k)\right)\\ W_T(k-N_{tx}/2)\exp\left(j2\pi nk/N_{tx}\right)\end{pmatrix}\\ \hat{\eta}_u^{(i)}(n)=\sqrt{1/N_{tx}}\sum_{k=0}^{N_{tx}-1}\hat{\Pi}_u^{(i)}(k)\exp\left(j2\pi nk/N_{tx}\right)\end{cases} \tag{13}$$

where $\mu_u^{(i)}(n)$, $\iota_u^{(i)}(n)$ and $\hat{\eta}_u^{(i)}(n)$ are the time-domain residual MUI, the residual ISI and the noise after performing MMSE-FDE, respectively. In this paper, $\mu_u^{(i)}(n)$ and $\iota_u^{(i)}(n)$ are approximated as zero-mean complex-valued Gaussian variable. The residual MUI plus the residual ISI plus noise component $\tilde{\eta}_u^{(i)}(n)=\mu_u^{(i)}(n)+\iota_u^{(i)}(n)+\hat{\eta}_u^{(i)}(n)$ can be treated as a new zero-mean complex-valued Gaussian variable, therefore, Eq. (12) can be rewritten as

$$\tilde{r}_u^{(i)}(n)=(A_u^{(i)}/\sqrt{2})\left(d_u(n)+d_u(n-1\ \mathrm{mod}.N_{tx})\right)+\tilde{\eta}_u^{(i)}(n)$$

Approximating that $\{\tilde{\eta}_u^{(i)}(n);n=0\sim N_{tx}-1\}$ are independent zero-mean complex-valued Gaussian variables, *a posteriori* probability of $d_u=[d_u(0),d_u(1),\ldots,d_u(N_{tx}-1)]$ for the given MUI cancellation output signal block $\tilde{r}_u^{(i)}=[\tilde{r}_u^{(i)}(0),\tilde{r}_u^{(i)}(1),\ldots,\tilde{r}_u^{(i)}(N_{tx}-1)]$ can be expressed as

$$p(d_u\,|\,\tilde{r}_u^{(i)})=\prod_{n=0}^{N_{tx}-1}p(d_u(n)\,|\,\tilde{r}_u^{(i)}(n)) \tag{15}$$

The log-likelihood ratio (LLR) for the *x*th bit (*x*=0~log$_2$*M*–1, where *M* is the modulation level) in the *n*th symbol $d_u(n)$ is computed as [10]

$$\begin{aligned}\Lambda_{u,x}^{(i)}(n)&=\ln\left[\sum_{d_u\in X:b_{n,x}=1}p(d_u\,|\,\tilde{r}_u^{(i)})\Big/\sum_{d_u\in X:b_{n,x}=0}p(d_u\,|\,\tilde{r}_u^{(i)})\right]\\ &\approx\ln\left[\max_{d_u\in X:b_{n,x}=1}p(d_u\,|\,\tilde{r}_u^{(i)})\right]-\ln\left[\max_{d_u\in X:b_{n,x}=0}p(d_u\,|\,\tilde{r}_u^{(i)})\right]\end{aligned} \tag{16}$$

where $\sum_{d_u\in X:b_{n,x}=1}p(d_u\,|\,\tilde{r}_u^{(i)})$ and $\sum_{d_u\in X:b_{n,x}=0}p(d_u\,|\,\tilde{r}_u^{(i)})$ are *a posteriori* probability summation of symbol candidates when transmitted bit $b_{n,x}$ is $b_{n,x}$ = 1 and $b_{n,x}$ = 0, respectively. In case of QPSK (*M*=4 and *x*=0,1) data modulation, an estimated symbol block $\{\tilde{d}_u^{(i-1)}(n);n=0\sim N_{tx}-1\}$ is given by [11]

$$\tilde{d}_u^{(i-1)}(n)=\sqrt{1/2}\left(\tanh\left(\Lambda_{u,0}^{(i-1)}(n)/2\right)+j\tanh\left(\Lambda_{u,1}^{(i-1)}(n)/2\right)\right) \tag{17}$$

Then, $N_{tx}$-point DFT is applied to transform the estimated symbol block $\{\tilde{d}_u^{(i-1)}(n);n=0\sim N_{tx}-1\}$ into frequency-domain components $\{\tilde{D}_u^{(i-1)}(k);k=0\sim N_{tx}-1\}$ as

$$\tilde{D}_u^{(i-1)}(k)=\sqrt{1/N_{tx}}\sum_{n=0}^{N_{tx}-1}\tilde{d}_u^{(i-1)}(n)\exp\left(-j2\pi kn/N_{tx}\right) \tag{18}$$

## 3.1 Parallel interference cancellation

In this subsection and the next subsection, we explain how to generate MUI replica and residual ISI replica of the *u*-th users at the *i*-th stage. In FD-IPMUIC, a series of

MMSE-FDE, frequency-domain MUI cancellation, and SOVA is carried out for all users at the same time. The MUI replica $\tilde{M}_u^{(i)}(k)$ and residual ISI replica $\tilde{I}_u^{(i)}(k)$ are generated by using $\tilde{D}_{u-1}^{(i-1)}(k)$, $\tilde{D}_{u+1}^{(i-1)}(k)$ and $\tilde{D}_{u}^{(i-1)}(k)$ as

$$\tilde{M}_u^{(i)}(k) = \begin{cases} \sqrt{\dfrac{2E_{s,u-1}}{T_s}} \begin{pmatrix} \tilde{D}_{u-1}^{(i-1)}(k+N_{tx}-m)W_T(k+N_{tx}/2-m) \\ H_{u-1}(k+N_{tx}-m)W_{R,u}^{(i)}(k) \end{pmatrix} & k=0\sim m-1 \\ \sqrt{\dfrac{2E_{s,u+1}}{T_s}} \begin{pmatrix} \tilde{D}_{u+1}^{(i-1)}(k-N_{tx}+m)W_T(k-3N_{tx}/2+m) \\ H_{u-1}(k-N_{tx}+m)W_{R,u}^{(i)}(k) \end{pmatrix} & k=N_{tx}-m\sim N_{tx}-1 \\ 0 & otherwise \end{cases} \tag{19}$$

and

$$\tilde{I}_u^{(i)}(k) = \left(\sqrt{2E_{s,u}/T_s}\,H_u(k)W_{R,u}^{(i)}(k) - A_u^{(i)}\right)W_T(k-N_{tx}/2)\tilde{D}_u^{(i-1)}(k) \tag{20}$$

Note that the users at the edge of total uplink spectrum, i.e. the 0th and the $U$−1th user, are suffered by the MUI of one adjacent user, where the rest are affected from two adjacent users.

### 3.2 Successive interference cancellation

In FD-ISMUIC, users are prioritized according to their instantaneous received SINR, where the $u$-th user's SINR $\gamma_u$ is given by

$$\gamma_u = \frac{E_{s,u}\left((1/N_{tx})\sum_{k=0}^{N_{tx}-1}H_u(k)W_T(k-N_{tx}/2)\right)}{\begin{pmatrix} E_{s,u-1}\left((1/m)\sum_{k=0}^{m-1}H_{u-1}(k+N_{tx}-m)W_T(k+N_{tx}/2-m)\right) \\ +E_{s,u+1}\left((1/m)\sum_{k=0}^{m-1}H_{u+1}(k)W_T(k-N_{tx}/2)\right)+N_0 \end{pmatrix}} \tag{21}$$

The received SINR $\{\gamma_u; u=0,\ldots,U-1\}$ are compared and users are ranked in the descending order. Here, we assume $\gamma_0 \geq \gamma_1 \geq \cdots \geq \gamma_{U-1}$ without loss of generality. The signal detection is done in the descending order of $\gamma_u$, where the MUI replica $\tilde{M}_u^{(i)}(k)$ is given by

$$\tilde{M}_u^{(i)}(k) = \begin{cases} \sqrt{\dfrac{2E_{s,u-1}}{T_s}} \begin{pmatrix} \tilde{D}_{u-1}^{(i)}(k+N_{tx}-m)W_T(k+N_{tx}/2-m) \\ H_{u-1}(k+N_{tx}-m)W_{R,u}^{(i)}(k) \end{pmatrix} & k=0\sim m-1 \\ \sqrt{\dfrac{2E_{s,u+1}}{T_s}} \begin{pmatrix} \tilde{D}_{u+1}^{(i-1)}(k-N_{tx}+m)W_T(k-3N_{tx}/2+m) \\ H_{u-1}(k-N_{tx}+m)W_{R,u}^{(i)}(k) \end{pmatrix} & k=N_{tx}-m\sim N_{tx}-1 \\ 0 & otherwise \end{cases} \tag{22}$$

and ISI replica is exactly the same as Eq. (20).

### 3.3 MMSE-FDE weight

The MMSE-FDE weight $\{W_{R,u}^{(i)}(k), k=0\sim N_{tx}-1\}$ at the $i$-th iteration is designed to minimize the mean-square error (MSE) between the frequency-domain signal after MUI cancellation $\tilde{R}_u^{(i)}(k)$ and the frequency-domain transmit signal $S_u(k)$. $W_{R,u}^{(i)}(k)$ is given as Ref. [8]

$$W_{R,u}^{(i)}(k) = \begin{cases} \dfrac{E_{s,u}H_u^*(k)}{\begin{pmatrix} E_{s,u}\rho_u^{(i-1)}|H_u(k)|^2+N_0 \\ +E_{s,u-1}\rho_{u-1}^{(i-1)}|W_T(k+N_{tx}/2-m)H_{u-1}(k+N_{tx}-m)|^2 \end{pmatrix}} & k=0\sim m-1 \\ \dfrac{E_{s,u}H_u^*(k)}{\begin{pmatrix} E_{s,u}\rho_u^{(i-1)}|H_u(k)|^2+N_0 \\ +E_{s,u+1}\rho_{u+1}^{(i-1)}|W_T(k-3N_{tx}/2+m)H_{u+1}(k-N_{tx}+m)|^2 \end{pmatrix}} & k=N_{tx}-m\sim N_{tx}-1 \\ E_{s,u}H_u^*(k)\Big/\left(E_{s,u}\rho_u^{(i-1)}|H_u(k)|^2+N_0\right) & otherwise \end{cases} \tag{23}$$

for FD-IPMUIC, and

$$W_{R,u}^{(i)}(k) = \begin{cases} \dfrac{E_{s,u}H_u^*(k)}{\begin{pmatrix} E_{s,u}\rho_u^{(i-1)}|H_u(k)|^2+N_0 \\ +E_{s,u-1}\rho_{u-1}^{(i)}|W_T(k+N_{tx}/2-m)H_{u-1}(k+N_{tx}-m)|^2 \end{pmatrix}} & k=0\sim m-1 \\ \dfrac{E_{s,u}H_u^*(k)}{\begin{pmatrix} E_{s,u}\rho_u^{(i-1)}|H_u(k)|^2+N_0 \\ +E_{s,u+1}\rho_{u+1}^{(i-1)}|W_T(k-3N_{tx}/2+m)H_{u+1}(k-N_{tx}+m)|^2 \end{pmatrix}} & k=N_{tx}-m\sim N_{tx}-1 \\ E_{s,u}H_u^*(k)\Big/\left(E_{s,u}\rho_u^{(i-1)}|H_u(k)|^2+N_0\right) & otherwise \end{cases} \tag{24}$$

for FD-ISMUIC, where

$$\rho_u^{(i-1)} = (1/N_{tx})\sum_{n=0}^{N_{tx}-1}\left\{1-|\tilde{d}_u^{(i-1)}(n)|^2\right\} \tag{25}$$

which represents the reliability of the transmit replica.

## 4 Computer simulation

Simulation parameter setting is shown in Table I. We assume QPSK data modulation, data symbol block size per user $N_{tx}$=64, number of symbols per block $N_c$=256, CP length $N_g$=16, and block Rayleigh fading channel having symbol-spaced $L$=16-path with uniform power delay profile. Ideal channel estimation and ideal slow transmit power control (TPC) (i.e. $E_{s,u}$=$E_s$ for all $u$) are also assumed. A single-cell with $N_c/N_{tx}$ users is assumed in this paper for simplicity. All users' signals are assumed to be received by the base station receiver at the same timing.

**Table I** Computer Simulation Parameters

| | | |
|---|---|---|
| Transmitter | Modulation | QPSK |
| | Number of symbols per block | $N_{tx}$=64 |
| | FFT/IFFT block size | $N_c$=256 |
| | GI size | $N_g$=16 |
| | Filter | Duobinary PR filter<br>Ideal brick-wall filter |
| Channel | Fading type | $L$=16-path block Rayleigh fading |
| | Power delay profile | Uniform |
| | Time delay | $\tau_l=l$ ($l$=0~$L$−1) |
| Receiver | Channel estimation | Ideal |
| | Equalization | FD-IPMUIC, FD-ISMUIC |

## 4.1 BER performance

BER performances of duobinary PR filtered SC-FDMA with FD-IPMUIC and FD-ISMUIC are plotted in Fig. 3 as a function of the average received bit energy-to-AWGN noise power spectral density ratio $E_b/N_0$, defined as $E_b/N_0=(1/\log_2 M)(E_s/N_0)(N_c+N_g)/(N_c-1)$. We assume $m$=16 in both FD-IPMUIC and FD-ISMUIC. BER of single-user case ($m$=0) is also plotted for comparison. It can be seen from Fig. 3 that as the number of iterations increases, FD-IPMUIC and FD-ISMUIC significantly improve the BER performance, where the BER is very close to single-user case ($I$=3). In addition, FD-ISMUIC provides better BER performance than FD-IPMUIC since successive approach improves accuracy of MUI replicas.

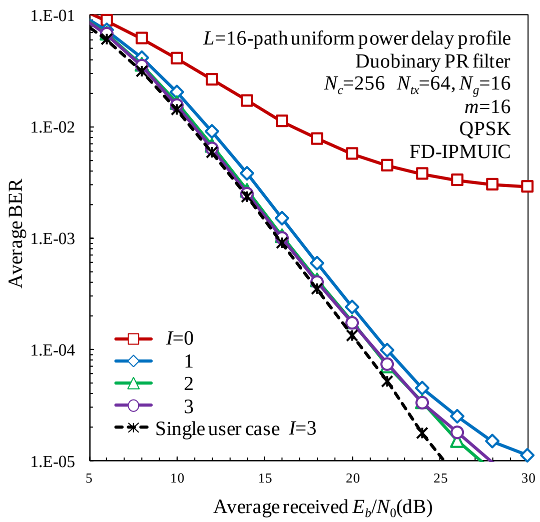


**(a)** FD-IPMUIC

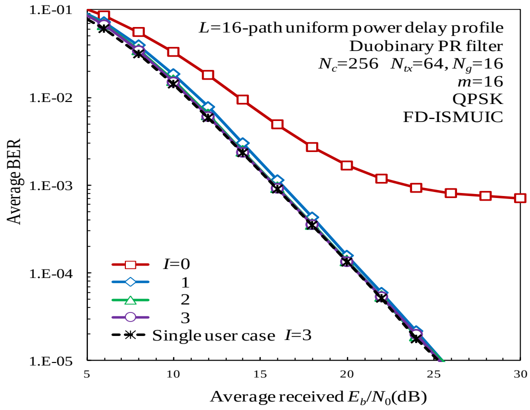


**(b)** FD-ISMUIC

**Figure 3** BER performance

## 4.2 Throughput performance

Throughput η(bps/Hz) is defined as

$$\eta = (1/\beta)\times \mathrm{lb}\, M \times (1-\mathrm{PER})\times(N_c-1)/(N_c+N_g) \qquad (26)$$

where PER represents packet error rate. PER is measured when FD-IPMUIC (FD-ISMUIC) with $I$=3, where a packet consists of 1024 information bits. The throughput performance is plotted as a function of β and $m$ in Fig. 4, where the average received $E_s/N_0$ is 23 dB. It is previously stated that SE can be improved when $m$ increases, however, the MUI simultaneously increases. From Fig. 4, the maximum throughput of transmission using FD-IPMUIC (FD-ISMUIC) is 1.937 (2.025) bps/Hz at $m$=16 (18), implying that the optimum spectrum overlapping for FD-IPMUIC and FD-ISMUIC are $m$=16 and 18, respectively.

The throughput performance is plotted as a function of average received $E_s/N_0$ in Fig. 5, where $m$=16 (18) for FD-IPMUIC (FD-ISMUIC). For comparison, the throughput is also plotted for Ideal brick-wall filtered SC-FDMA with ISI cancellation [8]. It can be seen that duobinary PR filtered FD-IMUIC can achieve higher throughput performance compared with ideal brick-wall filtered SC-FDMA with ISI cancellation in a certain $E_s/N_0$ range (between 22 dB and 25 dB). Duobinary PR filtered FD-ISMUIC can achieve higher throughput performance compared with FD-IPMUIC.

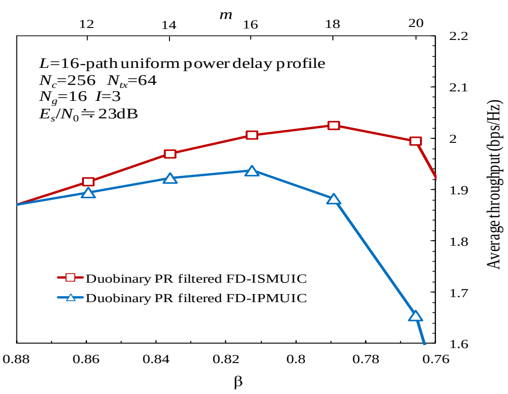


**Figure 4** Impact of β

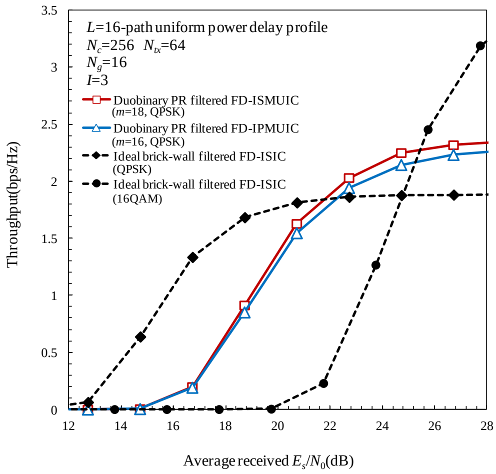


**Figure 5** Throughput performance

## 5 Conclusions

In this paper, we proposed two types of frequency-domain MUI cancellation technique, i.e., FD-IPMUIC and FD-ISMUIC, for duobinary PR filtered SC-FDMA uplink. FD-IPMUIC and FD-ISMUIC can sufficiently suppress MUI and achieve a BER performance close to the single-user case. Due to improved accuracy of MUI replicas achieved by successive cancellation approach, FD-ISMUIC provides better throughput performance than FD-IPMUIC. It was shown that FD-ISMUIC and FD-IPMUIC provide higher throughput than ideal brick-wall filtered SC-FDMA with ISI cancellation in a certain $E_s/N_0$ range (between 22 dB and 25 dB).

## References


[1] J. G. Proakis and M. Salehi, *Digital Communications*, 5th ed., McGraw-Hill, 2008.

[2] H. Sari, G. Karam, and I. Jeanclaude, “Transmission Techniques for Digital Terrestrial TV Broadcasting,” IEEE Communications Magazine, Vol. 33, pp. 100-109, Feb. 1995.

[3] D. Falconer, S. L. Ariyavisitakul, A. Benyamin- Seeyar, and B. Edison, “Frequency domain equalization for single-carrier broadband wireless systems,” IEEE Commun. Mag., Vol. 40, No. 4, pp. 58-66, Apr. 2002.

[4] F. Adachi, D. Garg, S. Takaoka, and K. Takeda, “Broadband CDMA techniques,” IEEE Wireless Commun. Mag., Vol. 12, No.2, pp. 8-18, Apr. 2005.

[5] Y. Akaiwa, *Introduction to digital mobile communication*, Wiley, New York, 1997.

[6] P. Kabal and S. Pasupathy, “Partial-response signaling,” IEEE Trans. Commun., Vol. 23, No. 9, pp. 921-934, Sept. 1975.

[7] K. Abo, A. Boonkajay, T. Yamamoto, and F. Adachi, “Duobinary PR response filtered SC-FDE,” Proc. The 10th IEEE Vehicular Technology Society Asia Pacific Wireless Communications Symposium (APWCS 2013), Seoul, Korea 22–23 Aug. 2013.

[8] S. Okuyama, K. Takeda, and F. Adachi, “Iterative MMSE-FDE/MUI Cancellation and Antenna Diversity for Frequency-Domain Filtered SC-FDMA Uplink,”, IEICE Trans. Commun., Vol. E94-B, No. 10, pp.2847-2856, Oct., 2011.

[9] J. Hagenauer and P. Hoeher, “A Viterbi algorithm with soft-decision outputs and its application,” IEEE GLOBECOM 1989, pp.1680-1686, Nov. 1989.

[10] M. P. C. Fossorier, F. Burkert, S. Lin and J. Hagenauer, “On the equivalence between SOVA and Max-Log-MAP decodings,” IEEE Commun. Letters, vol. 2, No. 5 pp.137-139, May 1998.

[11] K. Takeda, K. Ishihara, and F. Adachi, “Frequency-domain ICI cancellation with MMSE equalization for DS-CDMA downlink,” IEICE Trans. Commun., Vol.E89-B, No.12, pp.3335-3343, Dec. 2006.